

# 637 IMPACT OF RADIOSONDE MEASUREMENT ACCURACY ON PRECIPITATION TYPE AND CONVECTIVE WEATHER FORECAST

Raisa Lehtinen<sup>1\*</sup>, Petteri Survo<sup>1</sup>, Johanna Lentonen<sup>1</sup>, Mona Kurppa<sup>2</sup>  
<sup>1</sup> Vaisala Oyj, Helsinki, Finland, <sup>2</sup> University of Helsinki, Helsinki, Finland

## 1. INTRODUCTION

Radiosondes provide continuous, accurate profiles of temperature, humidity and wind from the ground up to the altitude of 35 km. This information is central input to numerical weather prediction (NWP) models. In addition, radiosondes have an important role in forecasting, model validation, climatology, atmospheric research, and validation of remote sensing instruments. These applications demand high accuracy and consistency of the measurement. However, the quality of the sensor measurements can affect the radiosonde's capability to correctly detect important details, such as temperature inversions, cloud layers, and ice formation layers, which are all essential for weather prediction.

This study evaluates and quantifies the impact of small measurement inaccuracies on the assessment and forecast of weather, with particular focus on convective weather and winter precipitation. The analysis includes a set of 56 Vaisala RS92 and RS41 soundings from three geographical regions during severe convective weather outbreaks. The impact of measurement accuracy was studied by modifying radiosonde profiles with small artificial temperature and humidity offsets and evaluating the changes in meteorological stability indices, using the original profiles as the reference. Sensitivity of winter precipitation type to data accuracy was explored similarly by examining baseline sounding profiles and simulated profiles in which small errors were introduced. The results demonstrate that small errors in vertical profile measurements can potentially lead to significant forecast errors during high-impact weather events.

## 2. FORECASTING CONVECTION USING RADIOSONDE PROFILES

### 2.1 Interpretation of radiosonde profiles

During convection, warm air near the ground starts rising, potentially leading to thunderstorms. Convection is still poorly represented in the NWP models due to inadequate spatial and temporal resolutions and the difficulty to quantify humidity distribution in the atmosphere. High-quality radiosonde profiles

show the characteristic features that predict the strength of the convection, including temperature inversions, wind shear, and cloud layers, and give the basis for understanding how the weather will evolve. These characteristics are illustrated in Figure 1 and discussed in the following.

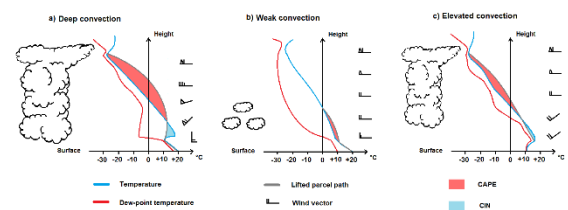


**Figure 1.** Model radiosonde profiles of temperature, dew-point and wind, predicting various types of convection.

### a) Deep convection

The air near the surface is warm, moist and well-mixed. There is a strong temperature inversion and enough convective inhibition (CIN) to prevent convection from beginning too early and thus enables convective available potential energy (CAPE) to build up. A relatively rapid decrease in temperature with height in the middle troposphere results in small stability. Cloud layers affect the amount of solar warming on the surface. Vertical wind shear is a main ingredient for severe and long-lasting thunderstorms.

### b) Weak convection

Only weak convection and small cumulus clouds occur if the boundary layer is not moist enough, there is not enough convective inhibition to help build up convective energy, and the mid-troposphere is too stable for thunderstorms to appear.

### c) Elevated convection

Thunderstorms can develop by means of elevated convection even if the air near the

\* Corresponding author address:  
Raisa Lehtinen, Vaisala Oyj, P.O. Box 26,  
FI-00421 Helsinki, Finland,  
e-mail: raisa.lehtinen@vaisala.com

surface is very stable due to temperature inversion. The air above the stable layer has the required characteristics, and convection can occur if the unstable air becomes lifted, for example, mechanically by a weather front.

## 2.2 Meteorological Indices

Meteorological indices are calculated from radiosonde profiles and, in some cases, from surface observations. An index describes in a single value some aspect of the state of the atmosphere. For example, the Convective Available Potential Energy (CAPE) index gives an estimate of the amount of energy a parcel of air would have if lifted a certain distance vertically through the atmosphere. Most meteorological indices have been specifically developed to improve forecasting of deep convection and thunderstorms. Indices facilitate the interpretation of radiosonde profiles and can be used together with other information sources to make forecast decisions.

The potential for severe weather estimated by the indices is typically categorized as “weak”, “moderate”, or “strong”. Threshold values for the different categories are approximate and depend on the season and climate. Some indices have different calculation options; as an example, the calculation of CAPE can start from the surface or from a higher level where the convection updraft is expected to initiate.

INDEX	PURPOSE	UNIT	WEAK	MODERATE	STRONG
<b>BRN</b> Bulk Richardson Number <sup>1</sup>	Storm cell type	-	< 10 pulse type convection	10-50 supercells	> 50 multi-cells
<b>CAPE</b> Convective Available Potential Energy <sup>2</sup>	Deep moist convection (thunder)	J/kg	USA: < 500 Europe: < 100	USA: 500-2000 Europe: 100-1000	USA: > 2000 Europe: > 1000
<b>CIN</b> convective inhibition <sup>2</sup>	Will convection happen?	J/kg	< -50	> -50	
<b>DCAPE</b> Downdraft CAPE <sup>2</sup>	Downdraft strength	J/kg	< 500	500 – 800	> 800
<b>KI</b> K-index <sup>3</sup>	Instability	°C (K)	< 20	20 – 30	> 30
<b>LI</b> Lifted index <sup>4</sup>	Instability and thunder potential	°C (K)	USA: > -2 Europe: > 0	USA: -2 ... -4 Europe: 0 ... -2	USA: < -4 Europe: < -2
<b>SI</b> Showalter index <sup>5</sup>	Instability	°C (K)	> 0 showers	0 ... -3 thunder	< -3 severe thunder

**Table 1.** Summary of meteorological indices used in the study and their approximate threshold values. <sup>1</sup> (Weisman, 1982), <sup>2</sup> (ERS, 2011), <sup>3</sup> (George, 1960), <sup>4</sup> (Galway, 1956), <sup>5</sup> (Showalter, 1947).

Therefore, the optimal use of indices requires expertise of the local weather and of how to best apply the indices. To give some insight into the orders of magnitude for each index, approximate thresholds are shown in Table 1.

## 3. IMPACT OF RADIOSONDE MEASUREMENT ACCURACY ON METEOROLOGICAL INDICES

### 3.1 Experimental setup

This study focuses on a set of seven commonly used meteorological indices for predicting severe weather, as shown in Table 1.

To study the effect of measurement accuracy on stability indices, a set of 56 soundings performed with either Vaisala Radiosonde RS92 or RS41 were selected. The soundings took place on two continents, in Europe and in continental United States of America, under conditions that resulted in severe convective weather. All radiosonde profiles used in this analysis were acquired from the archive of the University of Wyoming (UWYO, 2015).

The impact of measurement accuracy was studied by modifying radiosonde profiles with small artificial errors and calculating the changes in meteorological indices, using the original profiles as the reference. Offset values of -2 %, -4 % and +2 % RH for the relative humidity and  $\pm 0.2$  °C for the temperature were chosen based on a previous WMO radiosonde intercomparison (Nash et al., 2011). The offset values represent typical statistical biases observed between the instruments in the intercomparison. However, the reported sounding by sounding variations showed substantially larger deviations. Therefore, the simulated error values in this study can be considered as conservative. The impact of wind measurement accuracy was not analyzed in this study.

Modifying the temperature and humidity values also changes the corresponding partial water vapor pressure  $e$  and the dew-point temperature  $T_d$  values which were therefore recalculated using the formulas of Wexler, modified by Hardy (Hardy, 1998) and the Magnus formula (Buck, 1981), respectively. These formulas were tested to be similar to the formulas used for the sounding data drawn from the archive of the University of Wyoming.

The initial and modified sounding profiles were analyzed with RAOB software version 6.3 (ERS, 2011). RAOB automatically calculates index values based on the sounding and plots the data on a thermodynamic diagram. A thermodynamic diagram shows the relationship between the

pressure, temperature and humidity content of air, and allows the determination of the characteristics of the air mass, e.g. stability, cloud layers, fronts and vertical wind shear.

### 3.2 Results for all radiosonde profiles

The mean index values and the mean relative and absolute changes due to humidity and temperature offsets applied to the original radiosonde measurements are presented in Table 2, including all 56 soundings in conditions of severe convective weather. The mean relative changes are also shown in Figure 2. For BRN, CAPE, CIN and LI, the surface-based values (sfc) were used in the analysis. For SI and CIN, only the mean absolute changes should be considered as the mean values are close to zero and their relative changes are exaggerated.

	<i>BRN<sub>sfc</sub></i>	<i>CAPE<sub>sfc</sub></i> (J kg <sup>-1</sup> )	<i>CIN<sub>sfc</sub></i> (J kg <sup>-1</sup> )	<i>DCAPE</i> (J kg <sup>-1</sup> )	<i>KI</i> (°C)	<i>LI<sub>sfc</sub></i> (°C)	<i>SI</i> (°C)
<b>MEAN VALUE</b>	110	2060	-34.3	800	31.7	-4.8	-0.9
<b>RH-2 %</b>	-13 %	-15 %	-46 %	+2 %	-3 %	+9 %	+41 %
	-15	-216	+4.7	+16	-0.8	+0.4	+0.3
<b>RH-4 %</b>	-27 %	-29 %	-86 %	+5 %	-6 %	+21 %	+91 %
	-30	-444	-14.6	+33	-1.8	+0.9	+0.7
<b>RH+2 %</b>	+18 %	+18 %	+34 %	-2 %	+4 %	-13 %	-58 %
	+18	+274	+6.2	-15	+1.0	-0.5	-0.4
<b>T-0.2 °C</b>	-2 %	-2 %	+3 %	-2 %	0 %	+2 %	+4 %
	-4	-41	+0.6	-14	-0.1	+0.1	+0.0
<b>T+0.2 °C</b>	+7 %	+6 %	+5 %	+3 %	+1 %	-4 %	-20 %
	+6	+43	+1.1	+18	+0.3	-0.1	-0.1

**Table 2.** Summary of results for all 56 soundings. Mean index values and mean relative (bolded) and absolute changes in index values due to humidity offsets of -2, -4 and +2 % RH, and temperature offsets of ±0.2 °C applied to the whole sounding profile.

In general, the applied humidity offsets seemed to affect the index values more than the temperature offsets. The only exception was DCAPE, for which the observed effects were comparable in magnitude. Furthermore, CAPE-based indices and CIN were the most affected indices. This could be expected, since the calculation of these indices is based on integrating the measurements from near the surface to the upper levels of the troposphere, and thus, the measurement error accumulates to the index value at every measurement level. By contrast, KI, LI, and SI indices, being based on measurement results from a few levels only, were less affected by the offsets.

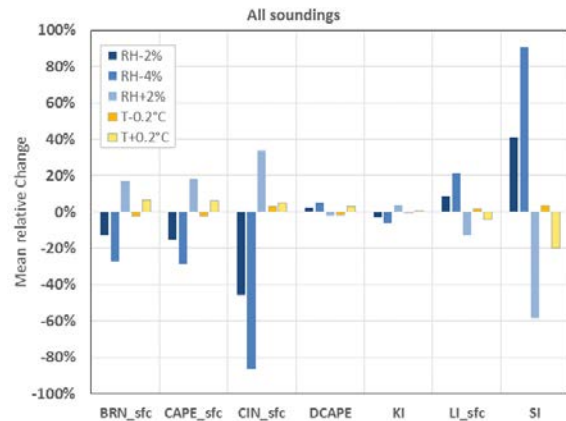


**Figure 2.** Mean relative changes in the studied indices due to relative humidity offsets of -4 to +2 % RH and temperature offsets of ±0.2 °C.

Humidity offsets resulted in both notable relative and absolute changes of  $CAPE_{sfc}$ , up to 29 % and 444 J/kg, respectively, for the -4 % RH offset. This was reflected in similar relative changes in  $BRN_{sfc}$ , which is directly proportional to  $CAPE_{sfc}$ . Also, the CIN index showed significant mean changes, up to -14.6 J/kg, due to the humidity offsets. In the case of  $LI_{sfc}$ , the relative changes were moderate, up to 21 %, whereas for DCAPE and KI the mean relative changes were weaker, within ± 6 %. SI values showed moderate absolute changes. Nevertheless, the interpretation of the SI value becomes clearly more uncertain due to the applied -4 % RH humidity offset.

As temperature profile modifications were studied, the added offsets of ±0.2 °C had a relatively weak impact on the studied indices, see Table 2 and Figure 2. The strongest effects were seen on  $BRN_{sfc}$  and  $CAPE_{sfc}$ , showing relative changes of 6 and 7 %, respectively. The seemingly large relative effect in SI can be considered weak when absolute scale is used in the interpretation of the results.

Figure 3 presents the distribution of absolute changes for  $CAPE_{sfc}$  and CIN index values as -4 % RH offset was added to the humidity profiles. Generally speaking, from the forecasting point of view, probably the most interesting CAPE range is from 500 to 2000 J/kg (highlighted data points) as these values indicate an increasing potential for the emergence of severe convective weather, see Table 1. The data shows that significant shifts, ranging typically from -500 to -250 J/kg, took place in this range. In addition, the CIN index shows decreased values with a large dispersion, especially around the critical range of -50 J/kg and below. Thus, as a consequence of -4 %RH offset, the combination of significantly lowered

CAPE value and the increased convective inhibition can lead to wrong conclusions of the evolving weather conditions.

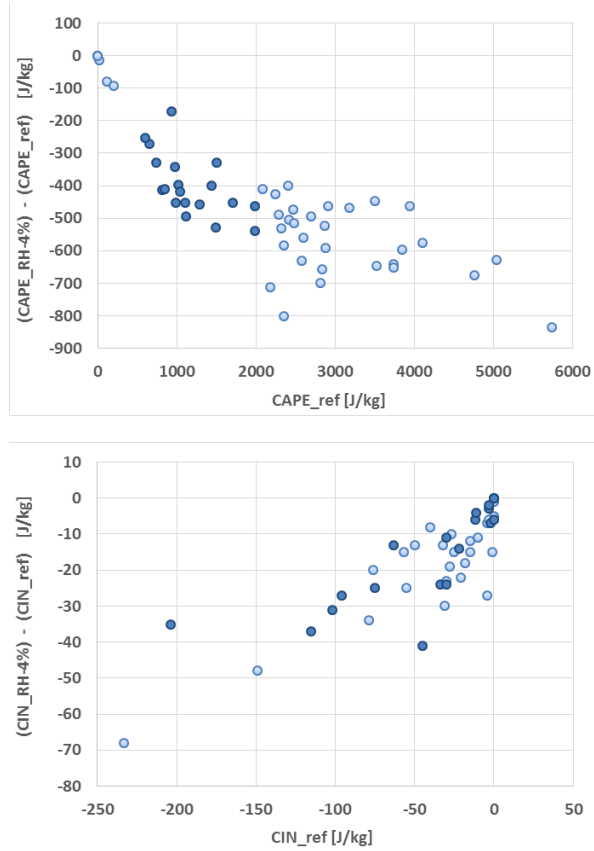


**Figure 3.** The absolute changes of  $CAPE_{srf}$  (top) and CIN (bottom) indices due to -4 % RH humidity offset as a function of the original index values. Data points corresponding to the critical CAPE range 500-2000 J/kg are highlighted.

### 3.3 Results for radiosonde profiles in weakly unstable atmospheric conditions

In order to study the impact of data accuracy in atmospheric conditions possessing less evident thunderstorm potential, the same analysis was conducted separately for 15 (out of 56) radiosoundings made in weakly unstable conditions, i.e. for profiles with  $CAPE_{sfc}$  less than 1000 J/kg. These conditions represent typical borderline cases where the analysis of the state of the atmosphere and the forecasts based on the indices are more uncertain and, consequently, either showers only or thunderstorms could be forecasted. The results for the chosen indices are shown in Table 3. Mean relative changes are also represented in Figure 4.

	$BRN_{sfc}$	$CAPE_{sfc}$ (J kg <sup>-1</sup> )	$CIN_{sfc}$ (J kg <sup>-1</sup> )	$DCAPE$ (J kg <sup>-1</sup> )	$KI$ (°C)	$LI_{sfc}$ (°C)	$SI$ (°C)
<b>MEAN VALUE</b>	26.8	458	-72.9	603	31.2	-0.9	0.6
<b>RH-2 %</b>	-21 %	<b>-30 %</b>	-27 %	+3 %	-3 %	<b>+17 %</b>	<b>+20 %</b>
	-5.7	-96	+0.6	+15	-0.8	+0.3	+0.3
<b>RH-4 %</b>	-43 %	<b>-49 %</b>	-72 %	+6 %	-6 %	<b>+34 %</b>	<b>+45 %</b>
	-10.5	-188	-23.4	+30	-1.7	+0.8	+0.7
<b>RH+2 %</b>	<b>+31 %</b>	<b>+34 %</b>	<b>+29 %</b>	-3 %	+3 %	<b>-13 %</b>	<b>-26 %</b>
	+7	+127	+9.3	-14	+0.9	-0.3	-0.4
<b>T-0.2 °C</b>	-3 %	-2 %	+3 %	-2 %	-1 %	+2 %	+3 %
	-1	-12	+0.9	-12	-0.1	+0.1	+0.1
<b>T+0.2 °C</b>	<b>+14 %</b>	<b>+20 %</b>	+3 %	+7 %	+1 %	-9 %	-9 %
	+3	+52	+2	+28	+0.2	-0.1	-0.1

**Table 3.** Summary of results for 15 soundings in which  $CAPE_{sfc} < 1000$  J kg<sup>-1</sup>. Mean index values and mean relative (bolded) and absolute changes in index values due to humidity offsets of -2, -4 and +2 % RH, and temperature offsets of  $\pm 0.2$  °C applied to the whole sounding profile.

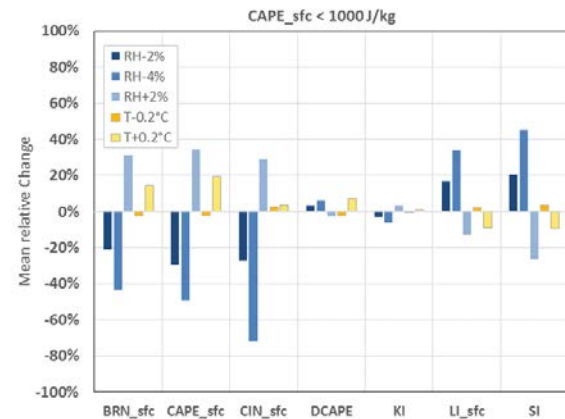


**Figure 4.** Mean relative changes of the studied indices due to relative humidity offsets of -4 to +2 % RH and temperature offsets of  $\pm 0.2$  °C. Results for the 15 soundings for which  $CAPE_{sfc} < 1000$  J/kg.

When comparing the analysis results of weakly unstable conditions with the results of all soundings, the most significant differences can be seen in the mean relative changes of  $BRN_{sfc}$  and  $CAPE_{sfc}$  indices. The changes due to the humidity offsets are nearly two-fold, up to 49 % on average for  $CAPE_{sfc}$ . In the absolute scale, the 188 J/kg mean reduction of the  $CAPE_{sfc}$  value by the -4 % RH offset is significant when compared to the original mean value 458 J/kg. For  $BRN_{sfc}$  the largest humidity offset shifts the mean index value from 26.8 to 16.3, making the interpretation of the index more ambiguous (see Table 1).



In weakly unstable conditions, the mean CIN index value,  $-72.9 \text{ J/kg}$ , was more than double the mean value of the analysis including all soundings, and the observed absolute change of  $-23.4 \text{ J/kg}$  was even more significant.

DCAPE and KI showed very similar results in the two analysis cases. The largest difference was seen in the mean relative change due to  $+0.2^\circ\text{C}$  temperature offset in DCAPE which shifted from  $+3\%$  to  $+7\%$ . However, the mean absolute change,  $+28 \text{ J/kg}$ , does not substantially impact the interpretation of the index.

For  $LI_{\text{sfc}}$  and SI, the absolute changes are similar to the previous analysis. However, this time the largest absolute change in  $LI_{\text{sfc}}$ ,  $+0.8^\circ\text{C}$ , is of the same order of magnitude as the initial mean index value,  $-0.9^\circ\text{C}$ .

As a summary of the analysis results, in weakly unstable atmospheric conditions most of the studied indices showed increased sensitivity to the applied artificial measurement errors. Evidently, in these borderline conditions, the accuracy of the weather forecast can be significantly degraded by the bias and random type measurement errors observed in WMO's previous radiosonde intercomparison.

#### 4. FORECASTING WINTER PRECIPITATION TYPE USING RADIOSONDE PROFILES

##### 4.1 Interpretation of Radiosonde Profiles

Winter weather forecasting is mainly focused on predicting the track and intensity of synoptic scale low-pressure systems, surface temperatures, and precipitation rate and type at the ground. Quantitative precipitation forecasting (QPF) is generally regarded as the least certain aspect in NWP models since very small changes in temperature or moisture can have a large effect on the type of precipitation. Radiosonde soundings play an important role in forecasting since they record many significant atmospheric features which, when assimilated into NWP models, help produce more accurate predictions. In addition, they help the forecaster understand situations where NWP models are known to be more uncertain, even misleading, and facilitate the interpretation of the upcoming precipitation type. The following discussion presents the six basic types of winter precipitation and how they can be predicted from radiosonde profiles, followed with a case example of a winter time radiosonde profile and its interpretation.

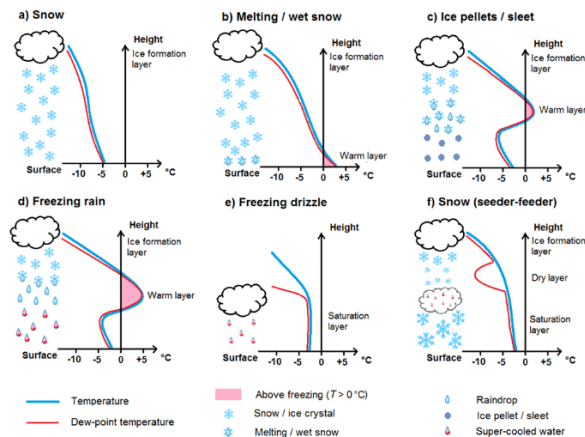


**Figure 5.** Illustrative radiosonde profiles of temperature and dew-point temperature, demonstrating characteristic features that correspond to various types of winter precipitation.

The six type of winter time weather conditions presented in Figure 5 can be described as follows. See also the terminology explanations in Table 4.

- a) Snowfall is observed when snow crystals are formed aloft in an ice formation layer and temperatures remain below freezing in the whole profile.
- b) If the surface layer temperature is above freezing, part of the falling snow flakes will melt to form melting (wet) snow.
- c - d) If ice particles fall through an elevated warm layer, they will melt partly or entirely. Depending on the degree of melting and the thickness of the adjacent near-surface cold layer, either ice pellets or freezing rain will be observed. Ice pellets are solid particles, while freezing rain consists of super-cooled liquid particles that partly freeze when in contact with a surface that is below freezing.
- e) If the saturation layer is shallow and below freezing, but warmer than  $-10^\circ\text{C}$ , freezing drizzle is likely to form.
- f) In a snow seeder-feeder mechanism ice particles are formed in an upper-level cloud, whereas a lower-level cloud contains only super-cooled water. Falling ice particles will partly sublimate in a dry layer between the clouds. If any ice particles reach the lower cloud, they will start to glaciare the super-cooled cloud droplets and snowfall will be observed.

Factor	Explanation	Interpretation of radiosonde profile
<b>Ice formation layer</b>	Formation of ice crystals and snow by heterogeneous nucleation when air is saturated relative to ice.	Ice formation (> 50% chance): T < -10 °C and air is saturated relative to ice.
<b>Warm layer (T &gt; 0 °C)</b>	Melting of ice or snow particles. Can be a surface layer or an elevated layer.	Warm layer maximum temperature Complete melting: Tmax > 3 °C Partial melting: Tmax = 1-3 °C No melting: Tmax < 1 °C
<b>Near surface layer</b>	Determines the precipitation type near and on the ground, and the possible formation of freezing rain, ice pellets, or sleet.	Snow: T_surface < 1 °C Ice pellets / sleet: T < -6 °C in a > 750 m layer Freezing rain: T < 0 °C in a < 750 m layer and on the ground
<b>Saturation layer</b>	A layer in which water vapor condensates or is deposited on particles. Indicates the depth of cloud layer and the type of precipitation.	Minimum layer depth for precipitation to form: > 500 m
<b>Dry layer</b>	A dry layer can block precipitation from reaching the ground due to evaporation aloft, or change the precipitation type due to cooling.	Maximum layer depth for precipitation to occur: ~ 1000-1500 m

**Table 4.** Factors affecting winter precipitation type and examples of their interpretation based on radiosonde profiles.

#### 4.2 Case Study: Freezing Rain and Ice Storm

This case study demonstrates the importance of accurate radiosonde observations in situations where NWP models are likely to be incorrect.

In January - February of 2014 the Eastern Europe, especially parts of Slovenia and Croatia, were exposed to long-lasting freezing rain conditions covering vast areas with ice. The extreme weather was caused by an encounter between cold arctic and moist subtropical air masses. Accumulation of ice damaged the power transmission network in both countries and large areas of forests were destroyed.

Temperature and humidity observations from a Vaisala Radiosonde RS92 launched at the Zagreb sounding station in Croatia on February 5, 2014, are presented in Figure 6. Light freezing rain was observed at the station during the soundings.

The radiosonde profile shows an elevated inversion layer with relatively dry and warm air at 900 hPa, and a saturated layer between 750 and 640 hPa. The mid-tropospheric air is dry and the surface layer is not saturated. There is a shallow ice formation layer at above 700 hPa,

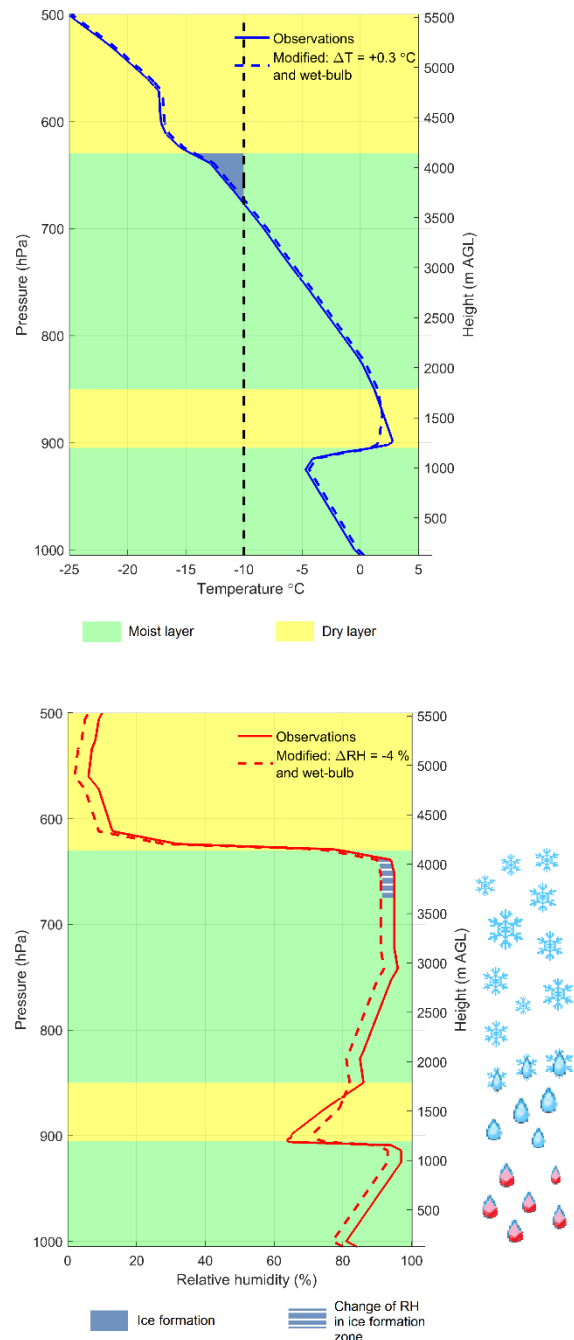


**Figure 6.** Radiosonde observations of temperature (top) and relative humidity with respect to ice (bottom), showing original measurements (solid lines) and modified profiles (dashed lines). In contrast to the actual study, here the modified profile combines both the offset and wet-bulb errors. The precipitation types for moist (green) and dry (yellow) layers according to the original measurements are illustrated on the right.

and the warm layer has a maximum temperature of 2.8 °C. In this case it is not obvious whether precipitation will fall in liquid or partly solid form. It is probable that ice formation will not be efficient enough, clouds will contain mostly

super-cooled water, and freezing rain will be observed on the ground.

In this type of borderline situation, even small temperature and humidity offsets can change the forecast towards either solid or liquid precipitation. The impact of measurement quality was studied by introducing a wet-bulb type error to the lowest dry layer, or alternatively, small offsets of +0.3 °C and -4 % RH, as shown by the dashed lines in Figure 6. Table 5 compares forecast results for the original and for the modified sounding profiles, using interpretation rules from Table 4.

Sounding profile	Modified sounding: wet-bulb error	Original sounding	Modified sounding: $\Delta T = +0.3$ °C, $\Delta RH = -4$ %
Ice formation	Shallow layer $T < -10$ °C → Probable ice formation	Shallow layer $T < -10$ °C → Probable ice formation	Shallow layer $T < -10$ °C → Less probable ice formation due to lower humidity
Elevated warm layer	$T_{max} = 1.9$ °C → Partial melting of ice → Solid and liquid can occur	$T_{max} = 2.8$ °C → Partial melting of ice → Rain more probable, also sleet can occur	$T_{max} > 3$ °C → Complete melting of ice → Rain
On the ground	$T_{surface} < 0$ °C → Rain will freeze on the ground → Ice accumulation or sleet	$T_{surface} < 0$ °C → Rain will freeze on the ground → Ice accumulation or sleet	$T_{surface} > 0$ °C → No freezing on the ground
Relative effect	---	Reference	+++
FORECAST	Ice pellets (more probable) or freezing rain or mix	Light freezing rain (more probable) or ice pellets	Light rain or no rain
OBSERVED WEATHER	Light freezing rain		

**Table 5.** Forecasts based on the original sounding profile and two modified profiles introducing a wet-bulb error (left) and temperature and humidity offsets (right). The table shows the reasoning based on factors in the sounding profiles, example forecasts, and the weather observation at the sounding site.

In these conditions a wet-bulb type error would decrease the level of melting in the elevated warm layer and thus increase the probability of ice pellet type of precipitation instead of freezing rain. On the other hand, a -4 % RH humidity offset would further decrease the efficiency of ice formation in the originally shallow ice formation layer. Combined with a temperature offset of +0.3 °C, which indicates a surface temperature above freezing, the forecasted precipitation type would more likely be rain.

## 5. SUMMARY

Among the upper air observation systems, radiosondes provide a unique set of data by producing complete vertical profiles describing the state of the atmosphere. This information is essential in determining the initial state of numerical weather prediction models. Furthermore, meteorologists are interested in several phenomena visible in the radiosonde profiles, including cloud layers, dry layers, temperature inversions, cold and warm fronts, jet streams, and wind shear. Radiosondes also have an important role in providing long-term high-quality time series of climatology trends in various parameters. All these applications set a high demand on the accuracy and consistency of the radiosonde measurements.

By utilizing the analysis of artificially modified radiosonde profiles, this study demonstrates that even small errors in vertical profile measurements may lead to erroneous forecast conclusions. The analysis of 56 radiosonde profiles preceding severe convective weather showed a 5 - 29 % mean relative change in key meteorological indices from a constant -4 % RH offset in humidity. The sensitivity to measurement error was even more significant in the borderline cases where the evolution of severe convection was more uncertain. A case study exploring winter forecasting demonstrates that a wet-bulb error or small humidity and temperature offsets of -4 % RH and +0.3 °C in the profile can change the forecasted precipitation type on the ground between ice pellets, freezing rain, and light rain.

Severe, high-impact weather conditions often imply a very challenging environment for the radiosonde sensors. The quality of the measurements determines the ability to detect important details properly. Reliable measurements and correct forecast decisions are paramount in such circumstances as the severe weather predictions have a large impact on the society.

## REFERENCES

- Bauman, W. H. I., Wheeler, M. M. & Short, D. A., 2005. Severe Weather Forecast Decision Aid, Kennedy Space Center, FL, USA, 50 pp: NASA Contractor Report CR-2005-121563.
- Buck, A., 1981. New equations for computing vapor pressure and enhancement factor. Journal of Applied Meteorology, Issue 20, pp. 1527-1532.
- ERS, 2011. RAOB: The Complete RAWinsonde OBServation Program. User Guide & Technical

Manual. Version 6.2. Environmental Research Services, LLC.

Gallus, B., 2008. Soundings as a tool to diagnose severe weather potential. Meteorology 416 - Lectures. Iowa State University. [Online] Available at: [http://www.meteor.iastate.edu/classes/mt417/powerpoint/417\\_wk6.pdf](http://www.meteor.iastate.edu/classes/mt417/powerpoint/417_wk6.pdf) [Accessed July 2015].

Galway, J. G., 1956. The lifted index as a predictor of latent instability. Bulletin of the American Meteorological Society, Issue 43, pp. 528-529.

George, J. J., 1960. Weather Forecasting for Aeronautics. Academic Press, Issue 673pp.

Hardy, B., 1998. ITS-90 formulations for vapor pressure, frostpoint temperature, dewpoint temperature, and enhancement factors in the range -100 to +100 C. Teddington, London England, The Proceedings of the Third International Symposium on Humidity & Moisture.

Nash, J., Oakley, T., Vömel, H. & Wei, L., 2011. WMO Intercomparison of high quality radiosonde systems. Yangjiang, China, 12 July - 3 August 2010, s.l.: WMO.

Puhakka, T., 1996. Ilmakehän termodynamiikka (in Finnish). Department of Meteorology, University of Helsinki. Title translation: Atmospheric thermodynamics.

Roine, K., 2001. Stabiilisuusindeksit ja sää Suomessa (in Finnish). Master's thesis, Department of Meteorology, University of Helsinki. Title translation: Stability indices and weather in Finland.

Savijärvi, H., 2010. Mesometeorologia (in Finnish). Atmospheric sciences. Department of Physics. University of Helsinki. Title translation: Mesometeorology.

Showalter, A., 1947. A stability index for thunderstorm forecasting. Bulletin of the American Meteorological Society, Issue 34, pp. 250-252.

Skystef, 2015. Storm indices. SkyStef's weather page. [Online] Available at: <http://www.skystef.be/storm-indices.htm> [Accessed July 2015].

UWYO, 2015. Atmospheric Soundings. University of Wyoming. [Online] Available at: <http://weather.uwyo.edu/upperair/sounding.html> [Accessed June 2015].

Weisman, M. L. & Klemp, J. B., 1982. The dependence of numerically simulated convective storms on vertical wind shear and buoyancy. Monthly Weather Review, Issue 110, pp. 504-520.